Large Eddy Simulation of Partial Cavitation Around a 2D Plane-Convex Hydrofoil

Hidalgo V.*; Escaler X.**; Soto R.***; Valencia E.***; Cando E.*; Luo X.*

*Tsinghua University, State Key Laboratory of Hydro science and Engineering, Beijing, China

e-mail: `victor.hidalgo@epn.edu.ec`

**UPC, Centre for Industrial Diagnostics and Fluid Dynamics, Barcelona, España

e-mail: `escaler@mf.upc.edu`

***Escuela Politécnica Nacional, Mechanical Engineering Department, Quito, Ecuador

e-mail: `ricardo.soto@epn.edu.ec/esteban.valencia@epn.edu.ec`

Resumen: Investigaciones sobre la cavitación tienen una gran importancia económica en el campo de la maquinaria hidráulica. Durante más de 40 años, métodos de mecánica computacional de fluidos han sido para entender estos fenómenos y ayudar a mejorar los diseños de maquinarias y equipos, como el caso de bombas y turbinas hidráulicas. Sin embargo, la cavitación aparece en flujos con números de Reynolds grandes, por lo cual, los modelos tradicionales de turbulencia Reynolds-averaged Navier-Stokes (RANS) $k - \epsilon$ y $k - \omega$ no son capaces de capturar el fenómeno de burbujas en movimiento. Por lo cual, la presente investigación usa el modelo de turbulencia Large Eddy Simulation (LES) con métodos implícitos (ILES) y explícitos (ELES), para simular la cavitación alrededor de un perfil plano-convexo . La simulación CFD ha sido llevada a cabo usando el programa de código abierto OpenFOAM y lenguaje python para el procesamiento de datos. La investigación indica que ELES e ILES porporcionan resultados similares a resultados experimentales obtenidos en el túnel de cavitación de la École Polytechnique Fédérale de Lausanne (EPFL).

Palabras claves: Cavitación, ILES, LES, OpenFOAM, Python.

Abstract: Investigations of attached partial cavitation are important because to prevent damages in hydrulic machinery and to reduce the costs. As expected computational fluid dynamics (CFD) methods have been developed for more than 40 years to understand this phenomenon and to improve the machinery designs, as pumps and hydraulic turbines. However, cavitation appears at high Reynolds numbers, so that, the traditional turbulence models Reynolds-averaged Navier-Stokes (RANS) $k - \epsilon$ and $k - \omega$ are not able to capture the bubbles motion. Therefore, large eddy simulation with implicit (ILES) and explicit (ELES) turbulence methods have been used to capture and study partial cavitation around a plane-convex hydrofoil. The CFD simulation has been carried out by the free open source software OpenFOAM and python language for data analysis. The research shows that ELES and ILES give results similar to experiments from the cavitation tunnel of the École Polytechnique Fédérale de Lausanne (EPFL).

Keywords: Cavitation, ILES, LES, OpenFOAM, Python.

1. INTRODUCTION

One of the main goals of Ecuador government is to transform the electricity generation matrix form thermal generation to hydraulic generation, which is aimed to increase up to 70%, as indicated in the studies of Hidalgo et al. [1]. As expected, a correct understanding of erosive cavitation could be used to prevent damage in turbines of hydropower stations [1]. However, the experiments to study cavitation are expensive and complex. In context, CFD seems a good alternative to study unsteady cavitation flows [2, 3].

Kubota et al. [4] presented a homogeneous model called bubble two phase flow (BTF), which is the basis of several numerical studies as indicated in Zhang et al.[5]. The main difficulty in most of the numerical studies is the RANS turbulence model, because it is not adequate to capture the unsteady behaviour of the sheet cav-

---

ity and cavitation shedding. Consequently, Ji et al. [6] used a modified turbulence model called the Partially-Averaged Navier-Stokes (PANS), which remarkably improved the RANS predictions. However, other authors have preferred to use LES as the estimated turbulence model [6, 7, 8], because in this model the large eddies are calculated and the small eddies are estimated based on a subrid model. Bensow and Liefvendahl [9] used ILES to avoid the explicit coupling between mass transfer modeling and subgrid modeling and compare with ELES for a marine propeller case. Their results show that ILES gives more similarity to experimental results than ELES. Thornber et al. [10] have shown that ELES has been successfully used for many prototype flows, however, this model provides excessive dissipation in flows from an initial perturbation to fully turbulent flow. Therefore, the use of ILES or ELES to study unsteady cavitanting flow around hydrofoils is a challenge that in the present article has been faced.

Finally the cavitation model of Zwart is an better option to study partial cavitation, it is not only an homogeneous model but also a no symmetrical condensation and evaporation model, as indicated in Hidalgo et al [11]. Thus Zwart model has been implemented in OpenFOAM for the present research.

2. MATHEMATICAL AND PHYSICAL DESCRIPTION

Two dimensionless numbers are necessary to describe cavitation conditions, which are Reynodls number, Re, and cavitation number, σ, as indicated in (1) and (2).

$$Re = \frac{U_\infty c}{\nu}, \tag{1}$$

$$\sigma = \frac{p_r - p_V}{\frac{1}{2}U_\infty^2 \rho}, \tag{2}$$

where U_∞ is the free stream velocity [12], c is the chord length, ν is the kinematic viscosity, p_r and p_V are the reference and the saturation pressures, respectively.

2.1 *Mathematics considerations for LES*

Equations (3) and (4) for continuity and momentum respectively are the basis of CFD simulations.

$$\frac{\partial \rho}{\partial t} + \frac{\partial (\rho u_i)}{\partial x_i} = 0, \tag{3}$$

$$\frac{\partial}{\partial t}(\rho u_i) + \frac{\partial}{\partial x_j}(\rho u_i u_j) = -\frac{\partial p}{\partial x_i} + \frac{\partial}{\partial x_j}\left[\rho \nu \left(\frac{\partial u_i}{\partial x_j} + \frac{\partial u_j}{\partial x_i}\right)\right], \tag{4}$$

where u is the instant velocity, ρf is the total volume force over a control volume, t is time, i and j are the space axes subindices.

However, the analytical method and direct method could not be used to solve (3) and (4). Therefore, the equations have been filtered to get (5) and (6) and solved by numerical methods.

$$\frac{\partial \rho}{\partial t} + \frac{\partial (\rho \overline{u_i})}{\partial x_i} = 0, \tag{5}$$

$$\frac{\partial}{\partial t}(\rho \overline{u_i}) + \frac{\partial}{\partial x_j}(\rho \overline{u_i u_j}) = -\frac{\partial \overline{p}}{\partial x_i} + \frac{\partial}{\partial x_j}\left[\rho \nu \left(\frac{\partial \overline{u_i}}{\partial x_j} + \frac{\partial \overline{u_j}}{\partial x_i}\right)\right]. \tag{6}$$

The following considerations are used to reduce (6) to (7):

1. The product of filtered velocities is $\overline{u_i u_j} = \overline{u_i}\,\overline{u_j} + \overline{u_i' u_j'}$.

2. The subgrid stress tensor, which is the Reynolds stress tensor is $\tau_{ij}' = \rho \overline{u_i' u_j'} = \rho(\overline{u_i u_j} - \overline{u_i}\,\overline{u_j})$.

3. The filtered strain tensor rate is $\overline{S}_{ij} = \frac{1}{2}\left(\frac{\partial \overline{u_i}}{\partial x_j} + \frac{\partial \overline{u_j}}{\partial x_i}\right)$.

4. The filtered viscous stress tensor is $\overline{\tau}_{ij} = 2\rho \nu \overline{S}_{ij}$.

$$\frac{\partial (\rho \overline{u_i})}{\partial t} + \frac{\partial (\rho \overline{u_i}\,\overline{u_j})}{\partial x_j} = -\frac{\partial \overline{p}}{\partial x_i} + \frac{\partial (\overline{\tau}_{ij} - \tau_{ij}')}{\partial x_j}. \tag{7}$$

2.2 *ELES considerations*

Smagorinsky model has been selected to do ELES, in which τ_{ij}' is considerer proportional to $\overline{S}_{ij}$ [8] that could be summarized as (8).

$$\tau_{ij}' - \frac{1}{3}\tau_{kk}\delta_{ij} = -2\rho \nu_{sgs}\overline{S}_{ij}, \tag{8}$$

where ν_{sgs} is the kinematic turbulent viscosity that models subgrid turbulence. It is modelled as (9).

$$\nu_{sgs} = (C_s\Delta)^2(2\overline{S}_{ij}\overline{S}_{ij})^{0.5}, \tag{9}$$

where C_s is the Smagorinsky constant that in OpenFOAM is calculated dynamically from the flow properties using Germano procedure [13] and Δ is defined as the cubic root of mesh cell volume.

Thus (7) is simplified by using the incompressibility constrain and the pressure has the trace term $\tau_{kk}\delta_{ij}/3$, as indicated in (10).

$$\frac{\partial \overline{u_i}}{\partial t} + \overline{u_j}\frac{\partial \overline{u_i}}{\partial x_j} = -\frac{1}{\rho}\frac{\partial \overline{p}}{\partial x_i} + \frac{\partial}{\partial x_j}\left([\nu + \nu_{sgs}]\frac{\partial \overline{u_i}}{\partial x_j}\right). \tag{10}$$

In addition for OpenFOAM, van Driest damping, is used to calculate the filter by (11)

$$\Delta = \min(\Delta_{mesh}, (k/C_{delta})y(1 - \exp(-y^+/A^+))), \quad (11)$$

where Δ_{mesh} is cubic root of the cell volume, k is von Kármán constant, $C_{delta} = 0.158$, $A^+ = 26$, y is the distance to the wall, and y^+ is the dimensionless number based on the wall shear stress [13].

2.3 *ILES considerations*

In ILES the subgrid stress tensor τ'_{ij} is expressed as indicated in (12).

$$\tau'_{ij} = \rho(\overline{\tilde{u}_i \tilde{u}_j} - \overline{\tilde{u}}_i \overline{\tilde{u}}_j + \tilde{\tau}'_{ij}), \quad (12)$$

where, the tensor $\tilde{\tau}'_{ij}$ is considered equal to subgrid dissipation scale action.

2.4 *Flow considerations*

Unsteady cavitating flows are caused by the pressure changes, so that, they are considered as multiphase flows with a two phase homogeneous mixture, as indicated from (13) to (15).

$$\alpha = \frac{\forall_V}{\forall}, \quad (13)$$

$$\rho = (1 - \alpha)\rho_L + \alpha\rho_V, \quad (14)$$

$$\mu = (1 - \alpha)\mu_L + \alpha\mu_V, \quad (15)$$

where α is the vapour void fraction, $\forall$ is the volume, V and L are subindices for vapour and liquid respectively, μ is the dynamics viscosity.

Based on multiphase flow considerations, α has been added to (5) to get (16).

$$\frac{\partial(\alpha\rho_V)}{\partial t} + \frac{\partial(\alpha\rho_V \overline{u}_i)}{\partial x_i} = \dot{m}, \quad (16)$$

where $\dot{m}$ is the interphase rate mass transfer per volume. Due to the mass transfer between phases, the velocity divergence has a no-homogeneous expression, as indicated in (17)

$$\frac{\partial \overline{u}_i}{\partial x_i} = \dot{m}\left(\frac{1}{\rho_V} - \frac{1}{\rho_L}\right). \quad (17)$$

2.5 *Zwart Cavitation Model*

Zwart model is based on Rayleigh Plesset's equation, but the second derivative term is neglected to obtain (18).

$$\frac{dR}{dt} = \sqrt{\frac{2}{3}\left(\frac{|p - p_V|}{\rho_L}\right)}. \quad (18)$$

Hence the Zwart expression is indicated in (19)

$$\dot{m} = \begin{cases} \dot{m}^+ = F_V \dfrac{3r_{\text{nuc}}(1 - \alpha)\rho_V}{R_B}\sqrt{\dfrac{2}{3}\left(\dfrac{p_V - p}{\rho_L}\right)} & if \ p < p_V \\[3mm] \dot{m}^- = -F_C \dfrac{3\alpha\rho_V}{R_B}\sqrt{\dfrac{2}{3}\left(\dfrac{p - p_V}{\rho_L}\right)} & if \ p > p_V \end{cases}, \quad (19)$$

where $F_V = 300$ and $F_C = 0.03$ are the selected calibration constants for vaporization and condensation based on the investigation of Morgout et al [14], $r_{\text{nuc}} = 5.0 \times 10^{-6}$ is the nucleation site volume fraction and $R_B = 1.9 \times 10^{-6}$ m is the typical bubble size in water [15].

It is noted that only the cavitation models of Kunz and Schnerr-Sauer are part of OpenFOAM solvers, so that, Zwart model has been compiled and implemented to OpenFOAM [15].

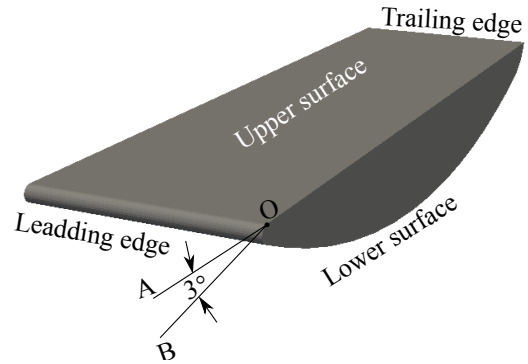## 3. DOMAIN SET UP

3.1 *Hydrofoil*

Figure 1. Plane-convex hydrofoil with 3° of attack angle $\widehat{AOB}$.

A plane-convex hydrofoil has been used in this research based on Escaler's studies [16], as indicated in Fig. 1. Fig. 2 shows the main CFD domain for the simulation, it is noted that the domain width is only 0.016c, so that, it can be considered a 2D simulation.

3.2 *Mesh*

A structured mesh has been elaborated with scale distribution around hydrofoil walls by GMSH, which is a free
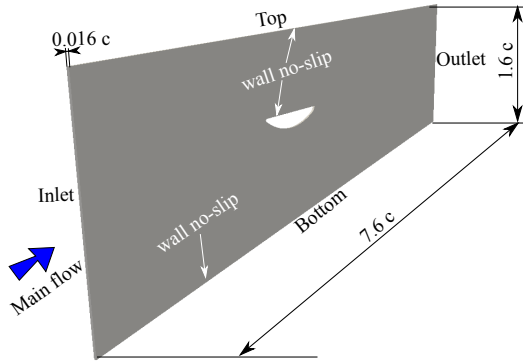
Figure 2. CFD domain with a width of 0.016c.
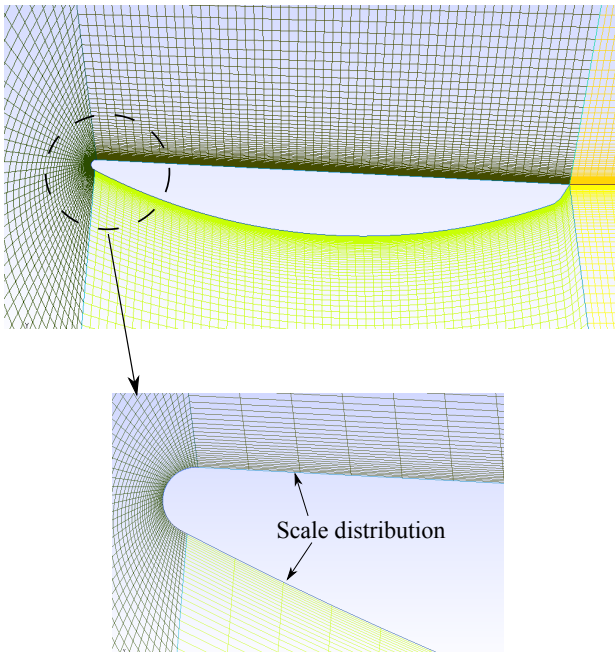
open source software [17], as shown in Fig. 3.

Figure 3. Structured mesh around the plane-convex hydrofoil.

The resulting mesh has 41024 quadrangles and 20011 hexahedra. y^+ is calculated based on (20) to guarantee the quality of mesh for ELES and ILES. The mean y^+ value of hydrofoil wall is about 9.46, which ensures that the mesh matches the conditions for ELES and ILES.

$$y^+ = \frac{u_\tau y}{\nu}, \tag{20}$$

where u_τ is the friction velocity and y is the distance to the nearest wall [15].

3.3 *OpenFOAM*

The OpenFOAM version 2.2.x has been used for the present study [12] in Ubuntu 14.04.1 LTS with kernel GNU/Linux 3.13. The Zwart cavitation model has been compiled and implemented following Hidalgo et al. [15] instructions.

3.4 *Boundary Conditions*

Table 1 shows the cavitation number, attack angle, mean flow stream velocity and average outlet pressure, which are the main boundary conditions for ELES and ILES based on the experiments carried out by Escaler [16].

Table 1. Boundary conditions.

Cases	σ	$\widehat{AOB}$	Inlet U_∞ (m/s)	Outlet P_r (kPa)
(a) ELES	1.0	3°	35.0	613.58
(b) ILES	1.0	3°	35.0	613.58

In addition the simulation time, t, has been set up to start from 0 seconds (s) to 0.05 (s), with a time interval of 1.5×10^{-6} (s).

4. RESULTS AND DISCUSSION

The local pressure coefficient, Cp, is calculated based on (21) and it has been plotted in Fig. 4 as a function of time to understand the behavior of the simulated flow.

$$Cp = \frac{p_s - p_r}{0.5U_\infty^2 \rho}, \tag{21}$$

where p_s is the local pressure over the hydrofoil upper surface.

Fig. 4 shows Cp as a function of $t(s)$ for a point located 0.14 x/c from leading edge for both ELES and ILES. Different behaviors, due to the number and periodicity of pulses. In context, ILES presents shorter cycles than ELES. Though ILES shows several groups of pulses every 0.01 (s) that are difficult to count, ELES presents two groups of pulses every 0.01 (s). So that, ELES presentd a more regular cyclic behavior than ILES. Finally, ILES predicts three times higher pulses than ELES.

In order to understand partial cavitation dynamics, typical cavitation cycles in each case, as indicated in Fig. 4. It is noted that intervals of time are different. Therefore, (22) is used to change time to dimensionless time.
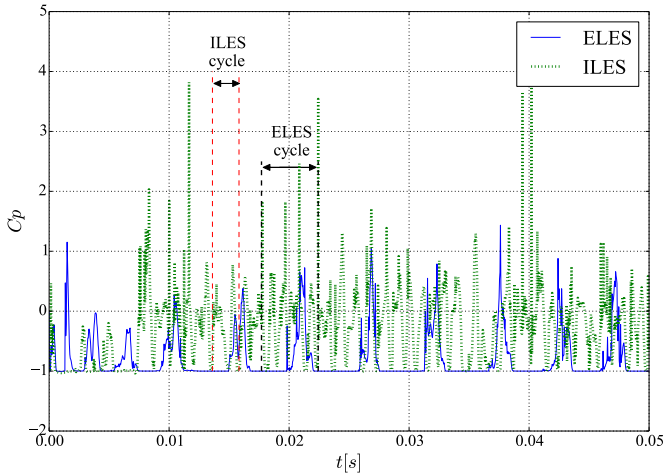
$$\zeta = \frac{t_f - t}{t_f - t_o} \tag{22}$$

Figure 4. Cp as a function of t (s) for a point located 0.14 x/c from leading edge.
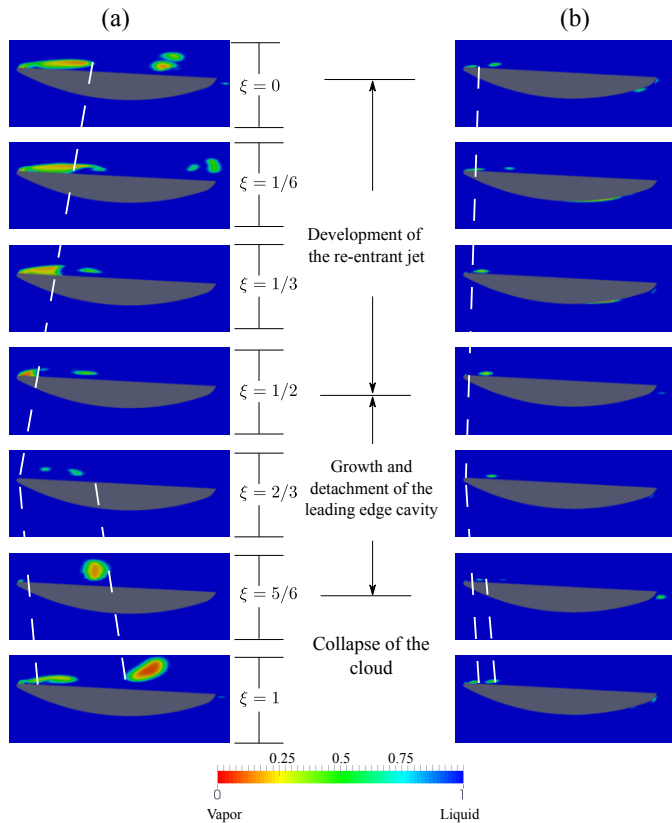

Figure 5. Typical cavitation cycles as a function of dimensionless time: (a) ELES and (b) ILES.

where t_o, t_f are the initial and final time of cavitation cycle respectively.

Fig. 5 shows the comparison between ELES and ILES for a typical cavitation cycle as a function of dimensionless

time. The following conclusions could be given:

1. The length of the cavity sheet, from $\xi = 0$ to $\xi = 1/2$ during the development of the re-entrant jet, is higher for ELES than ILES. This could be due to the fact that ELES provides excessive dissipation in unsteady flows [10].

2. During the growth and detachment of the leading edge cavity, both cases show similar behavior. However, ELES presents a cloud of bubbles at $\xi = 5/6$ close to the middle of the chord length than in ILES is a small cloud close to leading edge.

3. It is indicated from $\xi = 5/6$ to $\xi = 1$ that the cloud collapse in ILES is faster than in ELES. Therefore, this could be the reason that the shedding frequency is higher for ILES than ELES.

4.1 *Validation Case*

Fig. 6 has been processed by python language and it shows that ILES matches the experimental maximum length of the attached sheet of vapour (L_{max}) meanwhile ELES predicts more than two times L_{max}.
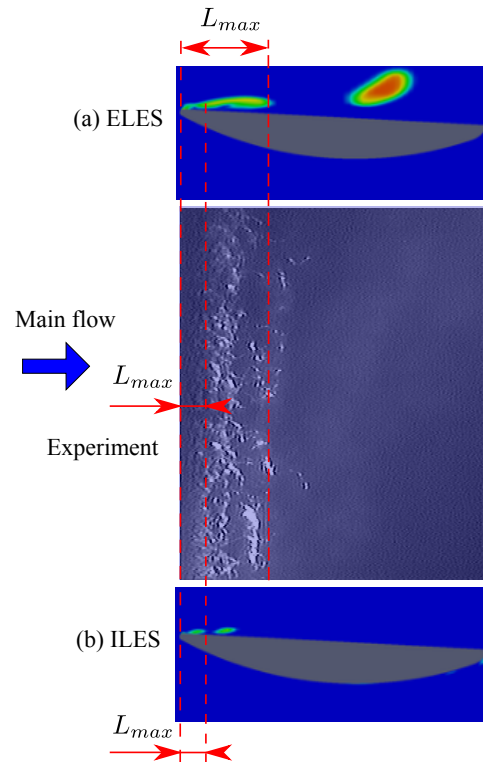

Figure 6. Comparison of the L_{max} of the experimental study with OpenFOAM results at $\xi = 1$.

L_{max}/c and the relative error with the experiment have been calculated to understand the differences between

OpenFOAM and experimental results as indicated in Table 2. As expected, ILES is more similar to experiments than ELES for the simulation of unsteady cavitating flows. Perhaps, if the subgrid model could be changed, the accuracy of ELES could be improved.

Table 2. Numerical study and experimental result based on L_{max}.

CASE	L_{max}/c		
	Num.	Exp.	% Error
(a) ELES	0.31	0.16	48.4
(b) ILES	0.14	0.16	12.5

5. CONCLUSIONS

In general, the present research has been served to simulate unsteady cavitating flows around a plane-convex hydrofoil. Explicit and implicit methods of large eddy simulation as turbulence model have been used, and the following milestones are the conclusions:

1. The Zwart cavitation model complied and implemented in OpenFOAM presents results close to experiments. In context, ILES appears a better option than ELES to study unsteady flows.

2. In summary, OpenFOAM, GMSH and python programming language are excellent tools for the numerical investigation of partial unsteady cavitation.

ACKNOWLEDGEMENTS

REFERENCES

[1] V. Hidalgo, X. Luo, A. Peña, E. Valencia, R. Soto, and A. Yu, "Benefits of hydropower research in Ecuador using OpenFOAM based on CFD technology (a practical cavitation study for NACA0015)," in *IX CONGRESO DE CIENCIA Y TECNOLOGÍA ESPE 2014*, pp. 123 – 127, ESPE, May 2014.

[2] V. Hidalgo and N. Chen, "Application of vortex process to cleaner energy generation," *Applied Mechanics and Materials*, vol. 71, pp. 2196–2203, 2011.

[3] V. Hidalgo, X. Luo, R. Huang, and E. Cando, "Numerical simulation of cavitating flow over 2d hydrofoil using openFOAM adapted for debian operating system with LXDE based in kernel GNU/Linux," in *Proceedings of the ASME 2014 4th Joint US-European Fluids Engineering*, pp. 1–8, 2014.

[4] A. Kubota, H. Kato, and H. Yamaguchi, "A new modelling of cavitating flows: A numerical study of unsteady cavitation on a hydrofoil section.," *Journal of fluid Mechanics*, vol. 240, no. 1, pp. 59 – 96, 1992.

[5] X. Zhang, W. Zhang, J. Chen, L. Qiu, and D. Sun, "Validation of dynamic cavitation model for unsteady cavitating flow on NACA66," *Science China Technological Sciences*, vol. 57, no. 4, pp. 819 – 827, 2014.

[6] B. Ji, X. Luo, Y. Wu, X. Peng, and Y. Duan, "Numerical analysis of unsteady cavitating turbulent flow and shedding horse-shoe vortex structure around a twisted hydrofoil," *International Journal of Multiphase Flow*, vol. 51, pp. 33–43, May 2013.

[7] N.-x. Lu, R. E. Bensow, and G. Bark, "LES of unsteady cavitation on the delft twisted foil," *Journal of Hydrodynamics, Ser. B*, vol. 22, no. 5, pp. 784–791, 2010.

[8] B. Huang, Y. Zhao, and G. Wang, "Large eddy simulation of turbulent vortex-cavitation interactions in transient sheet/cloud cavitating flows," *Computers & Fluids*, vol. 92, pp. 113–124, 2014.

[9] R. E. Bensow and M. Liefvendahl, "Implicit and explicit subgrid modeling in les applied to a marine propeller," in *38th Fluid Dynamics Conference and Exhibit*, American Institute of Aeronautics and Astronautics, 2008.

[10] B. Thornber and D. Drikakis, "The influence of initial conditions on turbulent mixing due to richtmyer-meshkov instability," *Journal of Fluid Mechanics*, vol. 654, pp. 99–139, 2010.

[11] V. Hidalgo, X. Luo, A. Yu, and R. Soto, "Cavitating flow simulation with mesh development using Salome open source software," in *Proceedings of the 11 th International Conference on Hydrodynamics (ICHD 2014)* (T. S. Keat, W. Xikun, G. W. Min, and J. CHUA, eds.), pp. 400 – 405, Nanyang Technological University, Singapore, Oct. 2014.

[12] V. Hidalgo, X. Luo, B. Ji, and A. Aguinaga, "Numerical study of unsteady cavitation on 2d NACA0015 hydrofoil using free/open source software," *Chin. Sci. Bull.*, pp. 1–7, June 2014.

[13] A. Krauze, A. Rudevics, A. Muiznieks, A. Sabanskis, N. Jekabsons, and B. Nacke, "Unsteady 3d LES modeling of turbulent melt flow with AC traveling EM fields for a laboratory model of the CZ silicon crystal growth system," in *International Scientific Colloquium Modelling for Electromagnetic Proceeding*, pp. 85,90, Oct. 2008.

[14] M. Morgut, E. Nobile, and I. Bilus, "Comparison of mass transfer models for the numerical prediction of sheet cavitation around a hydrofoil," *International Journal of Multiphase Flow*, vol. 37, July 2011.

[15] V. H. Hidalgo, X. W. Luo, X. Escaler, J. Ji, and A. Aguinaga, "Numerical investigation of unsteady cavitation around a NACA 66 hydrofoil using Open-FOAM," *IOP Conference Series: Earth and Environmental Science*, vol. 22, p. 052013, Dec. 2014.

[16] X. Escaler, M. Farhat, F. Avellan, and E. Egusquiza, "Cavitation erosion tests on a 2d hydrofoil using surface-mounted obstacles," *Wear*, vol. 254, no. 5, pp. 441 – 449, 2003.

[17] C. Geuzaine and J.-F. Remacle, "Gmsh: A 3-d finite element mesh generator with built-in pre- and post-processing facilities," *International Journal for Numerical Methods in Engineering*, vol. 79, no. 11, pp. 1309–1331, 2009.